Progress In Electromagnetics Research, Vol. 139, 41–55, 2013

THEORETICAL AND EXPERIMENTAL STUDY OF A MODULAR TUBULAR TRANSVERSE FLUX RELUCTANCE MACHINE

Dan-Cristian Popa*, Vasile-Ioan Gliga, and Loránd Szabó

Department of Electrical Machines and Drives, Technical University of Cluj-Napoca, 28 Memorandumului, Cluj-Napoca 400114, Romania

Abstract—There is an impetuous need for easy-to-build electrical machines with high specific thrust for various applications. The paper deals with a new modular variable reluctance tubular machine. It is a transverse flux machine without permanent magnets. Its construction is detailed and the novelty of the proposed structure is emphasized. A sample machine is analyzed by analytical and numerical means. The results of the analyses are validated by testing a laboratory model of the motor.

1. INTRODUCTION

The linear electrical machines gain more and more importance in various industrial applications, as transportation [1, 2], healthcare [3, 4], energy conversion [5] and several others [6, 7]. Most of the researches were focused on flat-type or tubular structures with permanent magnets (PMs) due to their high efficiency, high power/force density and excellent servo characteristics.

However, these machines have several disadvantages mainly related to the permanent magnets: environmental limitations (high temperature, corrosive surroundings), unsure availability of the magnets, the difficult manufacturing technology and high costs [8]. For these reasons, linear machines without PMs (especially variable reluctance types) could be of real interest in diverse industrial applications.

One of the major shortcomings of all flat-type linear machines is the great attraction force between the armatures, about ten times bigger than the traction tangential force [9]. This drawback

Received 8 March 2013, Accepted 11 April 2013, Scheduled 17 April 2013

* Corresponding author: Dan-Cristian Popa (Dan.Cristian.Popa@emd.utcluj.ro).

can be removed by considering two alternatives to the flat-type structures: double sided and tubular structures. However, a very precise adjustment of stator and moving armatures axes must be achieved. Otherwise the eccentricity faults could have a negative influence on the behavior of this cylindrical structure [10]. Some of the major advantages of tubular variable reluctance machines, both with open or closed magnetic circuit, are given in [11]. In [4], an application of a six phase machine, with longitudinal flux paths, driving a pump for heart assistance circulatory is reported. In [12], the performances of three and four-phase tubular linear stepping motors are analyzed. In [13], the authors of this paper studied a combination of a usual rotational switched reluctance machine (SRM) and a special linear SRM with several mover modules on its shaft that can perform both rotary and linear movement. One of the most important advantages of the tubular machines without PMs is given by the possibility to use them in high temperature environments where the absence of the PM becomes a significant advantage.

The authors have studied intensively the flat-type modular linear transverse flux reluctance machine, both with hybrid and electromagnetic excitation, with very similar performances of the two machines. Thus, a flat-type linear transverse flux motor with PM was presented in [14]. This machine with hybrid excitation was obtained as a combination between the already usual rotary variant of a PM transverse flux machine with passive rotor and a modular hybrid linear motor. In this case, the design, as for several rotary structures [15–17], had started from the volume of the PM needed in order to obtain the imposed force. In [18] a simpler structure, without PMs, was analyzed. A comparison between these variants was presented in [19], evidencing the similar characteristics. In the case of the machine with electromagnetic excitation, for a novel structure like the one studied there, such a design algorithm is considerable difficult to be created. However, it must be taken into account that this structure has the advantage over the one with PM of a lower mass and price and a less complicated construction.

The machine taken into study is the tubular variant of the above mentioned modular flat-type linear transverse flux reluctance machine with electromagnetic excitation. The basic elements of its structure and design algorithm, along with the results of the preliminary numerical analysis are given in [20]. A more detailed presentation of the modular tubular transverse flux reluctance machine (MTTFRM) is given in this paper. An analytical analysis based on the magnetic equivalent circuit and a numerical analysis using 3D FEM are performed here on a designed sample MTTFRM. A laboratory model of

the machine was built up. The performed experimental tests validated the results of the analyses.

The machine is suitable for applications where severe space and environmental limitations are imposed, or when high precision is required. The effectiveness of linear variable reluctance machines for such applications has been reported in [13, 21]. A short analysis concerning the employ of the proposed machine for such applications is also given in the paper.

2. THE MTTFRM STRUCTURE

The MTTFRM is a multiphase machine. The minimum number of the required N stator phases for a continuous movement is three [21]. The basic structure of the machine is given in Figure 1.

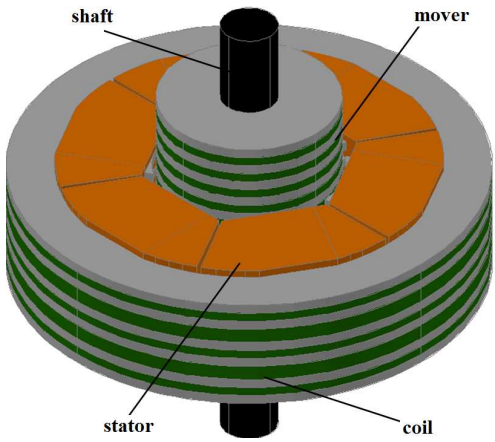

Figure 1. The structure of the MTTFRM.

A phase is composed of m magnetic pieces called axial teeth, Figure 2(a), alternating with $(m-1)$ non-magnetic spacers, Figure 2(b). An axial tooth is a module of the stator phase. Each module has Z poles and slots. The mover is passive. It consists of simple cylindrical magnetic pieces, called as well axial teeth, Figure 2(c), alternating with non-magnetic spacers, Figure 2(d). The core pieces can be made of both soft magnetic composites (SMC) and steel laminations.

The sum of the length of an axial tooth (t_s on the stator, t_m on the mover) and of a spacer (s_s on the stator and s_m on the mover) is the common tooth pitch τ, Figure 3. The lengths of the axial teeth on both armatures are equal.

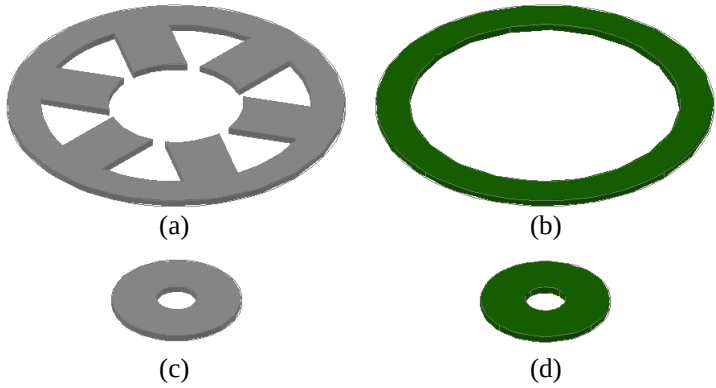

Figure 2. Parts of the stator and mover: (a) Stator core piece (axial tooth or module of the stator phase), (b) stator spacer, (c) mover core piece (axial tooth), (d) mover spacer.

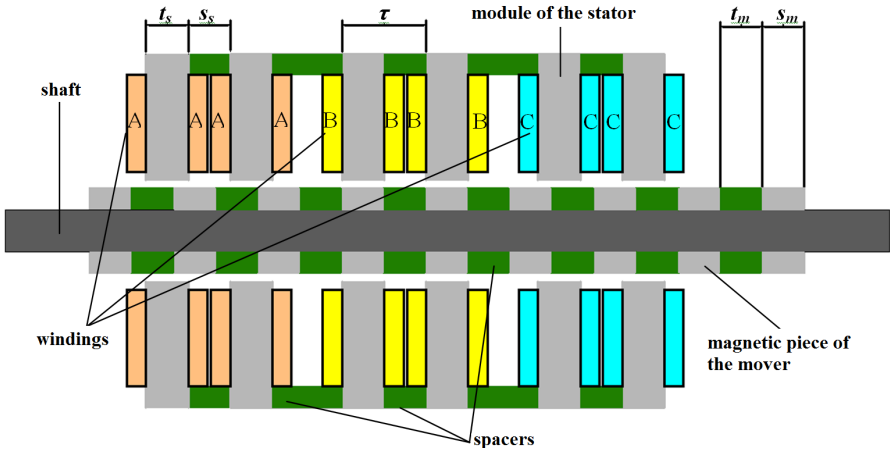

Figure 3. Longitudinal cross sectional view through of the MTTFRM.

In order to work properly the stator phases have to be shifted by $s_m + \tau/N$, which is assured by using proper non-magnetic spacers. The step length of the motor (d_i) depends on the pole pitch τ and the number of phases N:

$$d_i = \frac{\tau}{N} \tag{1}$$

The size notations of a magnetic piece are explained in a cross sectional view through the motor, Figure 4.

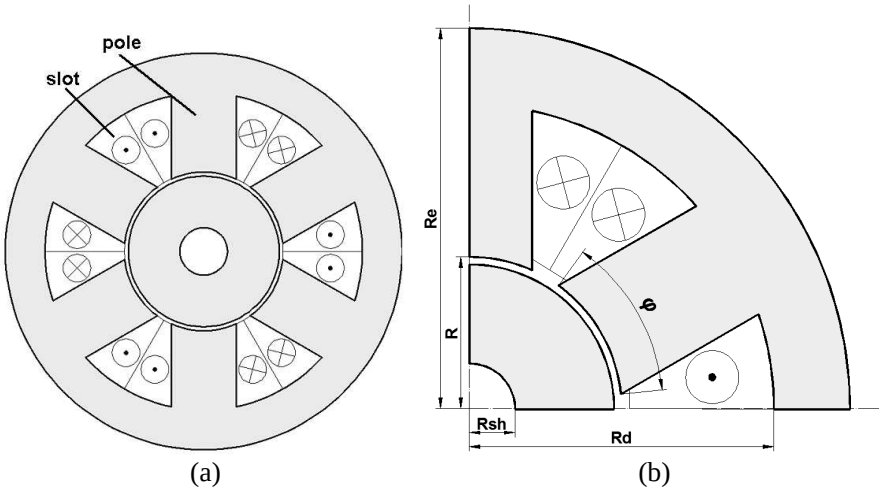

Figure 4. (a) Transverse cross sectional view through the proposed MTTFRM. (b) Dimensions of a module of a stator phase.

As shown in Figure 4(a), each module has an independent winding. Concentrated coils are used, as in the case of the SRM [22].

The windings of a phase, as well as the coils of a module, can be connected in series or in parallel. The advantage of a parallel connection is the increased fault tolerance of the motor [23].

When supplying a winding of a phase the teeth of that module will tend to align with the teeth of the mover. For the position given in Figure 3, in order to obtain a movement of the motor to the left, the succession in which the phases must be supplied is A, C, B. MTTFRM is controlled by a dedicated driver, similar to that used at a classical SRM. So, only a single phase is energized at each time and consequently only a single phase is generating traction force. The total force is the one given by one module multiplied by the number of modules of a phase.

The proposed MTTFRM can be used in precise positioning applications. Considering the requirements of such an application (imposed outer radius, rated supply voltage etc.) the basic starting design data were established. These data and some other necessary imposed design values are given in Table 1.

By applying the design algorithm detailed in [21] a sample MTTFRM was sized. The imposed design data of the MTTFRM are given in Table 2.

The next sections are dealing with the analytical, numerical and experimental analysis of the designed MTTFRM.

Table 1. Imposed design data.

Maximum traction force $f_{\max}$	120 N
Imposed speed v	0.75 m/s
Number of phases N	3
Number of modules of a phase m	2
Number of poles of a module Z	6
Air-gap flux density B_g	1.15 T
Step length d_i	3.33 mm
Outer radius R_e	125 mm
Air-gap length g	0.5 mm
Rated voltage U	12 V

Table 2. Geometric dimensions and other parameters of the designed machine.

Mean radius in the air-gap $R - g/2$	48 mm
Shaft radius R_{sh}	10 mm
Height of the stator pole h_p	40 mm
Yoke height $R_e - R_d$	32 mm
Stator pole angle φ	50°
Number of turns on a pole N_t	54
Rated current on a module of a phase I	10.2 A
Length of an axial tooth $t_s = t_m$	5 mm
Length of the stator l_s	61.67 mm
Length of the mover l_m	220 mm
Mass of the mover M_m	4.69 kg
Mass of the winding M_{Cu}	0.31 kg
Mass of the machine M_t	12.14 kg
Resistance of a coil of a module R_S	0.19 Ω
Inductance of a coil of an aligned module L_S	5.13 mH

3. ANALYTICAL ANALYSIS

The analytical analysis was performed by using the magnetic equivalent circuit (MEC) of a MTTFRM axial tooth of the stator and of the mover [24]. Despite the radial symmetry, the task to create a simplified MEC is difficult due to the influences of each pole on the

neighboring ones. Hence, a quite complex MEC is obtained, as shown in Figure 5.

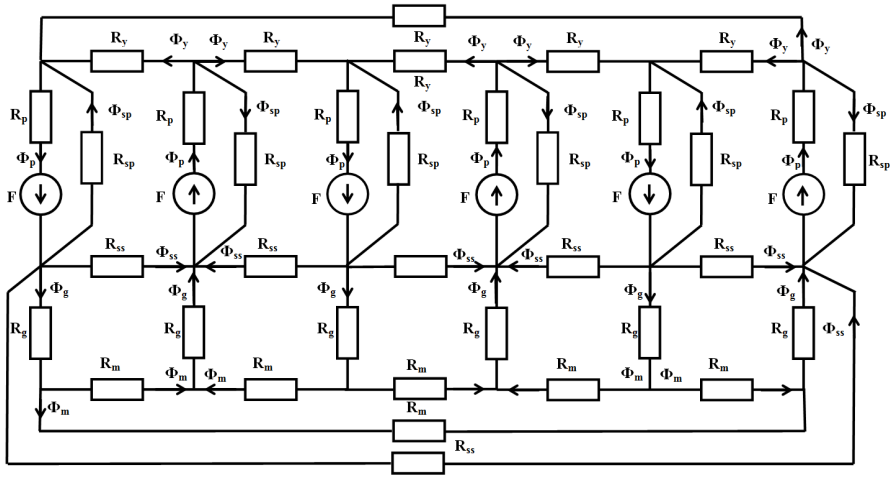

Figure 5. MEC of an axial tooth of the stator and of the mover.

The goal of the analysis is to compute the value of the air-gap flux density in the aligned position of the teeth of the two armatures and to compare it with the imposed one.

The flux densities in different parts of the machine (pole, yoke, mover, air-gap) have to be computed. The magnetic fluxes are computed by solving the equations system written by applying the Kirchhoff's laws for the MEC:

$$\begin{cases} \Phi_g + 2\Phi_{ss} + \Phi_{sp} - \Phi_p = 0 \\ \Phi_p - \Phi_{sp} - 2\Phi_y = 0 \\ \Phi_g - 2\Phi_m = 0 \\ 2\Phi_p R_p + \Phi_y R_y + \Phi_{ss} R_{ss} - 2F = 0 \\ \Phi_p R_p + \Phi_{sp} R_{sp} - F = 0 \\ 2\Phi_g R_g + \Phi_m R_m - \Phi_{ss} R_{ss} = 0 \end{cases} \tag{2}$$

The index notations used in (2) are: g — air-gap, p — pole of a module, y — yoke, m — mover, ss — leakage in the air-gap, sp — leakage between two neighboring poles. The fluxes obtained after solving the system are given in Table 3. The percentage values of the fluxes with respect to the flux through the pole, considered as the reference value, were calculated and are given in Table 3.

The resulted flux density values are presented in Table 4.

Table 3. Magnetic fluxes in different parts of the machine.

Flux	Value	Percentage
Φ_p	$0.3846 \cdot 10^{-3}$ Wb	100%
Φ_y	$0.1675 \cdot 10^{-3}$ Wb	43.66%
Φ_m	$0.1442 \cdot 10^{-3}$ Wb	37.59%
Φ_g	$0.2885 \cdot 10^{-3}$ Wb	75.01%
Φ_{sp}	$0.0233 \cdot 10^{-3}$ Wb	6.07%
Φ_{ss}	$0.0243 \cdot 10^{-3}$ Wb	6.33%

Table 4. Flux density values in different parts of the machine.

Flux density	Domain	Value
B_p	Pole	1.77 T
B_y	Yoke	1.01 T
B_m	Mover	0.82 T
B_g	Air-gap	1.08 T

The employed analytical analysis provided a value of the air-gap flux density close to the one imposed during the design.

4. NUMERICAL ANALYSIS OF THE MTTFRM

The performances of the designed MTTFRM were verified via finite element analysis (FEA). The complex three dimensional (3D) flux paths of the machine require a three-dimensional analysis [25]. Hence the magneto-static module from Cedrat's Flux 3D package was used [26].

Due to the radial symmetry, only a single stator pole of a module, the neighboring slots and the nearby mover part were modeled. However, it must be considered that the neighboring axial teeth of the mover have a significant influence on each other. From this reason the used geometric model, presented in Figure 6, consists of a single stator pole of a module, the neighboring slots and five mover corresponding parts and the non-magnetic spacers between them.

Based upon the results obtained with the simplified model, the solution for the entire structure has been computed in Flux 3D.

The mesh of the model has 107,464 nodes and 633,783 volume elements. The number of excellent quality elements is 63.37%, while the number of poor quality elements is 0.59%. These are very good

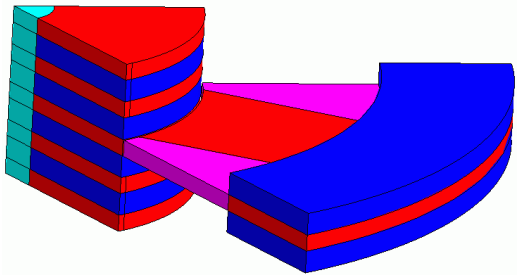

Figure 6. The applied Flux 3D model of the MTTFRM.

values of the mesh for a 3D model and assure fairly accurate results [26].

The FEA focused on computing the flux density distribution in the machine and the developed traction force. Next, the most significant results of the analysis are discussed.

The flux density map in the aligned position of the stator teeth with the mover teeth is given in Figure 7.

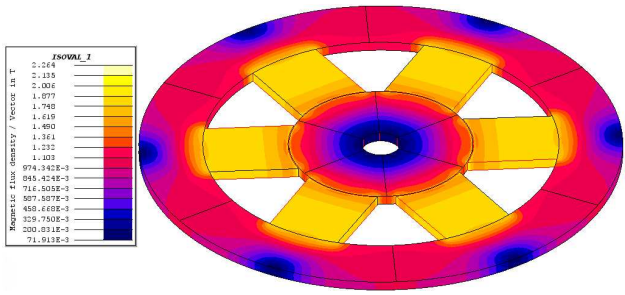

Figure 7. Flux density distribution in the aligned position of the stator and mover teeth.

The variation of the flux density modulus on radial direction (from inside to the exterior), in the aligned position of the teeth, is given in Figure 8. It can be seen that the flux density values in the pole, yoke and mover are close to the ones obtained via the analytical analysis.

The flux density in the air-gap, plotted along a circular arc with the radius equal to the mean radius of the air-gap is given in Figure 9. Due to the symmetry of the machine only the plot along the $1/Z$ of the total circumferential length has been plotted.

Both in Figures 8 and 9 the computed values are marked with black dots and the red curve was fitted to them. These numerical results are in good agreement with the data obtained via analytical computations.

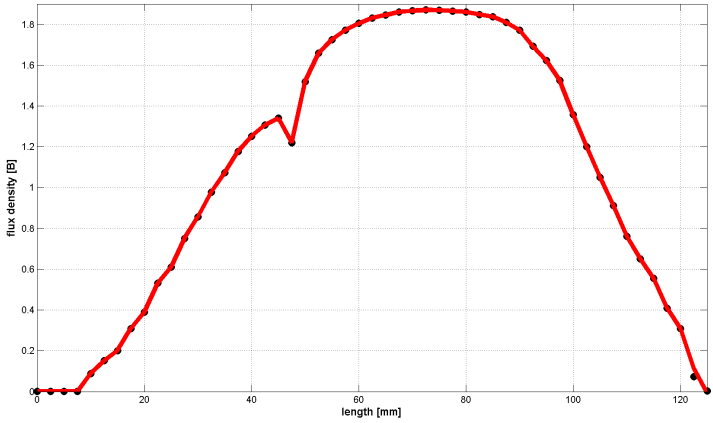

Figure 8. Flux density variation on the radial direction, from inside to exterior, in the aligned position of the two armatures.

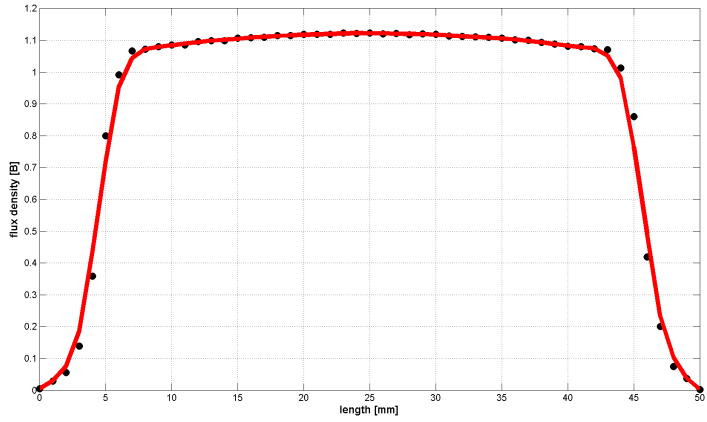

Figure 9. Flux density variation in the air-gap on the circumference, corresponding to a stator pole and its neighboring slots, in the aligned position of the armatures.

The traction force versus linear position static characteristic has been determined. The force was computed against a relative mover displacement equal to half of the pole pitch (5 mm). The step between two successive positions was 0.5 mm. It should be mentioned that the traction force is proportional with m and Z. The total force was calculated by multiplying the obtained value with Z and m. ($Z \cdot m = 12$ in the case of the machine in this study). In Figure 12, a

comparison between numerical and experimental static characteristic of the traction force is presented.

5. LABORATORY TESTS

The laboratory model of the designed MTTFRM was built. The main components of the machine are shown in Figure 10(a): (a) the shaft, (b) the mover, (c) the linear ball bearing, (d) the stator armature and (e) the inductive position transducer.

The assembled machine is presented in Figure 10(b).

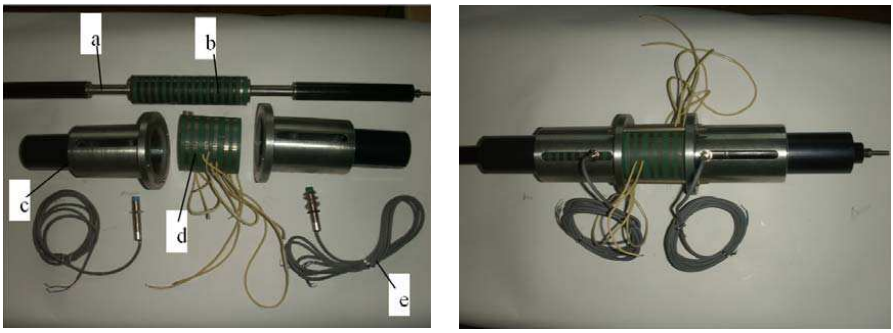

(a) (b)

Figure 10. The prototype of MTTFRM: (a) Component parts, (b) assembled machine.

In order to perform the static measurements, the test bench given in Figure 11 has been built. It consists of: (a) the MTTFRM, (b) auxiliary power supply, (c) PLC Controller, (d) motor power supply, (e) PIC controlled linear driver with firmware motor control software, (f) Fluke ScopeMeter used for signal display, (g) laptop for control and monitoring, (h) emergency stop push button, (i) HBM force sensor of PW6KC3MR type (20 kgf–500 R1).

The static characteristic of the traction force versus the linear displacement, plotted in Figure 12, was obtained using the force measurement system integrated in the laboratory setup.

As it can be seen, the experimental results confirmed the outcomes of the FEA. The small differences are due to measurement errors, construction inaccuracies and the use of magnetic materials with lower quality than of those designed.

Figure 11. The experimental setup.

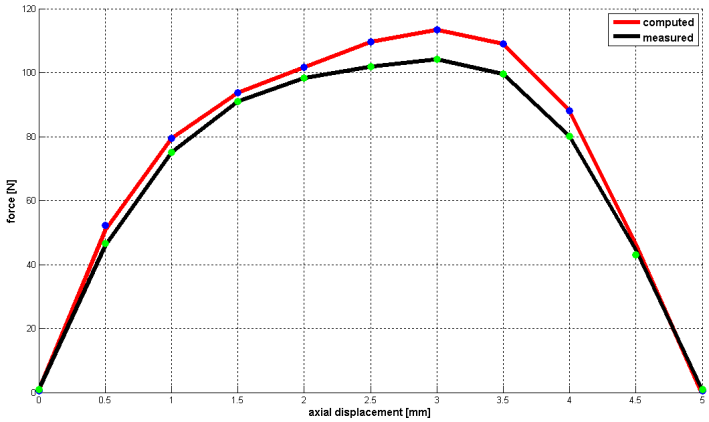

Figure 12. The static characteristic of the force on half of the pole pitch obtained from FEA and experiments.

6. CONCLUSIONS

A novel topology of a tubular motor with a modular construction was analyzed. Its innovative construction involves the alternative use of very simple magnetic and non-magnetic pieces for the core assembly. This allowed a smaller mass of the machine than using a compact iron core. Beside this advantage, the lack of the PMs led to a relative small price of the machine.

A good accordance between the analytical and numerical analyses of the flux densities in different parts of the iron core has been found. In order to obtain the variation of the force versus the displacement, the experimental tests were performed on a laboratory model. The static characteristics of the computed and measured traction forces

are relatively close. The maximum traction force developed by this low cost, small volume, simple machine has relatively great value.

The MTTFRM can be used in typical applications of the linear variable reluctance motors, such as precise position control, healthcare, robotics, advanced manufacturing systems, etc. It is also a good alternative to other conventional linear motors, with or without PMs.

ACKNOWLEDGMENT

This paper was supported by the project "*Development and support of multidisciplinary postdoctoral programmes in major technical areas of national strategy of Research — Development — Innovation*" 4D-POSTDOC, contract No. POSDRU/89/1.5/S/52603, project co-funded by the European Social Fund through Sectoral Operational Programme Human Resources Development 2007–2013.

REFERENCES

1. Yan, L., L. Zhang, T. Wang, Z. Jiao, C. Y. Chen, and I. M. Chen, "Magnetic field of tubular linear machines with dual Halbach array," *Progress In Electromagnetics Research*, Vol. 136, 283–299, 2013.
2. Wang, J., W. Wang, and K. Atallah, "A linear permanent-magnet motor for active vehicle suspension," *IEEE Transactions on Vehicular Technology*, Vol. 60, No. 1, 55–63, 2011.
3. Yamada, H., M. Yamaguchi, H. Kobayashi, Y. Matsuura, and H. Takano, "Development and test of a linear motor-driven total artificial heart," *IEEE Engineering in Medicine and Biology Magazine*, Vol. 14, No. 1, 84–90, 1995.
4. Llibre, J. F., N. Martinez, P. Leprince, and B. Nogarede, "Innovative linear pulsatile pump for heart assistance circulatory," *Proceedings of the 8th International Symposium on Linear Drives for Industrial Application*, Paper No. 207, on CD, Eindhoven, Netherlands, 2011.
5. Wang, J., M. West, D. Howe, H. Z.-D. La Parra, and W. M. Arshad, "Design and experimental verification of a linear permanent magnet generator for a free-piston energy converter," *IEEE Transactions on Energy Conversion*, Vol. 22, No. 2, 299–306, 2007.
6. Wang, J. and D. Howe, "Tubular modular permanent-magnet machines equipped with quasi-halbach magnetized magnets —

Part I: Magnetic field distribution, EMF, and thrust force," *IEEE Transactions on Magnetics*, Vol. 41, No. 9, 2470–2478, 2005.

7. Musolino, A., R. Rizzo, and E. Tripodi, "Tubular linear induction machine as a fast actuator: Analysis and design criteria," *Progress In Electromagnetics Research*, Vol. 132, 603–619, 2012.
8. Alonso, E., et al., "Evaluating rare earth element availability: A case with revolutionary demand from clean technologies," *Environmental Science & Technology*, Vol. 46, 3406–3414, 2012.
9. Boldea, I. and S. A. Nasar, *Linear Electric Actuators and Generators*, Cambridge University Press, 1997.
10. Torkaman, H. and E. Afjei, "Radial force characteristic assessment in a novel two-phase dual layer SRG using FEM," *Progress In Electromagnetics Research*, 185–202, 2012.
11. Tomczuk, B. and M. Sobol, "Field analysis of the magnetic systems for tubular linear reluctance motors," *IEEE Transactions on Magnetics*, Vol. 41, No. 4, 1300–1305, 2005.
12. Missaoui, W., L. El Amraoui, F. Gillon, M. Benrejeb, and P. Brochet, "Performance comparison of three and four-phase linear tubular stepping motors," *Proceedings of International Conference on Electric Machines*, Paper 467, on CD, Chania, Greece, 2006.
13. Szabó, L., I. Bentţia, D. C. Popa, and M. Ruba, "Contributions to the two degrees of freedom modular variable reluctance motors used in advanced manufacturing systems," *Proceedings of the IEEE International Conference on Automation, Quality and Testing, Robotics*, 093_85.pdf, on CD, Cluj-Napoca, Romania, 2012.
14. Popa, D. C., V. Iancu, and L. Szabo, "Linear transverse flux motor for conveyors," *Proceedings of the 6th International Symposium on Linear Drives for Industrial Application,* Paper 188, on CD, Lille, France, 2007.
15. Hanselman, D. C., *Brushless Permanent-magnet Motor Design*, McGraw-Hill, 1994.
16. Norhisam, M., S. Ridzuan, R. N. Firdaus, C. V. Aravind, H. Wakiwaka, and M. Nirei, "Comparative evaluation on power-speed density of portable permanent magnet generators for agricultural application," *Progress In Electromagnetics Research*, Vol. 129, 345–363, 2012.
17. Jian, L., G. Xu, Y. Gong, J. Song, J. Liang, and M. Chang, "Electromagnetic design and analysis of a novel magnetic-gear-integrated wind power generator using time stepping finite element method," *Progress In Electromagnetics Research*, Vol. 113, 351–

367, 2011.

18. Popa, D. C., L. Szabo, and V. Iancu, "Improved design of a linear transverse flux reluctance motor," *Proceedings of the 11th International Conference on Optimization of Electrical and Electronic Equipment*, Paper No. 399, 136–141, Braşov, Romania, 2008.
19. Szabo, L., I. A. Viorel, M. Ruba, and D. C. Popa, "Comparative study on different variable reluctance linear machine structures (with/without permanent magnets)," *Proceedings of the 6th International Symposium on Linear Drives for Industrial Application,* Paper 173, on CD, Lille, France, 2007.
20. Popa, D. C., V. I. Gliga, L. Szabo, and V. Iancu, "Tubular transverse flux variable reluctance motor in modular construction," *Proceedings of the 13th International Conference on Optimization of Electrical and Electronic Equipment*, 572–577, Braov, Romania, 2012.
21. Gan, W.C., G. P. Widdowson, M. S. W. Tam, and N. C. Cheung, "Application of linear switched reluctance motors to precision position control," *Asian Power Electronics Journal*, Vol. 2, No. 1, 31–36, 2008.
22. Krishnan, R., "*Switched Reluctance Motor Drives — Modeling, Simulation, Analysis, Design, and Applications*, Industrial Electronics Series, CRC Press, 2001.
23. Zhao, W., M. Cheng, R. Cao, and J. Ji, "Experimental comparison of remedial single-channel operations for redundant flux-switching permanent-magnet motor drive," *Progress In Electromagnetics Research*, Vol. 123, 189–204, 2012.
24. Matyas, A. R., K. A. Biro, and D. Fodorean, "Multi-phase synchronous motor solution for steering applications," *Progress In Electromagnetics Research*, Vol. 131, 63–80, 2012.
25. Mahmoudi, A, N. A. Rahim, and H. W. Ping, "Axial-flux permanent-magnet motor design for electric vehicle direct drive using sizing equation and finite element analysis," *Progress In Electromagnetics Research*, Vol. 122, 467–496, 2012.
26. FLUX 3D v11 User Manual, Cedrat, Meylan, France, 2009.